Photonic crystals: putting a new twist on light

J. D. Joannopoulos, Pierre R. Villeneuve & Shanhui Fan

Photonic crystals are materials patterned with a periodicity in dielectric constant, which can create a range of 'forbidden' frequencies called a photonic bandgap. Photons with energies lying in the bandgap cannot propagate through the medium. This provides the opportunity to shape and mould the flow of light for photonic information technology.

For the past 50 years, semiconductor technology has played a role in almost every aspect of our daily lives. The drive towards miniaturization and high-speed performance of integrated electronic circuits has stimulated considerable research effort around the world. Unfortunately, miniaturization results in circuits with increased resistance and higher levels of power dissipation, and higher speeds lead to a greater sensitivity to signal synchronization. In an effort to further the progress of high-density integration and system performance, scientists are now turning to light instead of electrons as the information carrier.

Light has several advantages over the electron. It can travel in a dielectric material at much greater speeds than an electron in a metallic wire. Light can also carry a larger amount of information per second. The bandwidth of dielectric materials is significantly larger than that of metals: the bandwidth of fibre-optic communication systems is typically of the order of one terahertz, while that of electronic systems (such as the telephone) is only a few hundred kilohertz. Furthermore, light particles (or photons) are not as strongly interacting as electrons, which helps reduce energy losses.

In spite of the numerous advantages of photons, all-optical circuits have yet to be commercially available on a large scale. Some hybrid optoelectronic circuits have produced significant improvement over the performance of electronic circuits, but the difficulties in designing a multipurpose optical component analogous to the electronic transistor has severely hindered the proliferation of all-optical systems. A new class of optical materials known as photonic crystals[1] may hold the key to the continued progress towards all-optical integrated circuits. Indeed, scientists have begun imagining photonic integrated circuits which resemble microscopic metropolises at micrometre length scales, with photonic crystal buildings that house bundles of light, and highways and bridges that guide light along narrow channels and around tight corners.

The underlying concept behind photonic-crystal materials stems from early ideas by Yablonovitch[2] and John[3]. In a nutshell, the idea is to design materials so that they can affect the properties of photons, in much the same way that ordinary semiconductor crystals affect the properties of electrons. Both Yablonovitch and John suggested that structures with periodic variations in dielectric constant could influence the nature of photonic modes in a material; Yablonovitch's aim was to control the radiative properties of materials, while John's was to effect photon localization[4–7] by introducing a random refractive-index variation.

Traditionally, the manipulation of optical photons has relied in general on the mechanism of total internal reflection. Light propagating in a high-dielectric material is reflected at the interface with a low-dielectric material. This severely limits the degree of miniaturization of optical components because the interface must be smooth with respect to the wavelength of light. Photonic crystals offer a completely different mechanism for the control of light. The difference lies in the concept of a photonic bandgap—the optical analogue of the electronic bandgap in semiconductors.

In a semiconductor, the atomic lattice presents a periodic potential to an electron propagating through the electronic crystal. Moreover, the geometry of the lattice and the strength of the potential are such that, owing to Bragg-like diffraction from the atoms, a gap in allowed energies opens up for which an electron is forbidden to propagate in any direction. In a photonic crystal, the periodic 'potential' is due to a lattice of macroscopic dielectric media instead of atoms. If the dielectric constants of the constituent media are different enough, Bragg scattering off the dielectric interfaces can produce many of the same phenomena for photons as the atomic potential does for electrons. Thus a photonic crystal could be designed to possess a complete photonic bandgap—a range of frequencies for which light is forbidden to exist within the interior of the crystal. Forbidden, that is, unless there is a defect in the otherwise perfect crystal. A defect, or mistake in the periodicity, could lead to localized photonic states in the gap, whose shapes and properties would be dictated by the nature of the defect. A point defect could act like a microcavity, a line defect like a waveguide, and a planar defect like a perfect mirror. This ability to manipulate a photon provides us with a new dimension in our ability to mould or control the properties of light. Therein lies the exciting potential of photonic crystals.

Of course, while the periodic arrangement of atoms occurs naturally in semiconductors, photonic crystals need to be fabricated artificially. To fully appreciate the challenge of fabricating these structures, we note that the lattice constant of the photonic crystal (that is, the size of the basic unit cell) must be comparable to the wavelength of the light. For the optoelectronics industry, for instance, where the usual operating frequency is around 1.5 μm (in the infrared), the lattice constant of a useful photonic crystal must be of the order of 0.5 μm. Although this is about 1,000 times larger than the lattice constant of atomic crystals, it is still over 100 times smaller than the diameter of a human hair. The fabrication of these intricate structures requires state-of-the-art microlithography techniques, such as electron-beam lithography and X-ray lithography.

From a theoretical point of view, the description of light in photonic crystals must involve the solution of Maxwell's equations in a periodic dielectric medium. An appealing aspect of Maxwell's equations is that, unlike the complex strongly interacting many-particle problem of electrons in a solid, they can be solved exactly. With linear materials there are no interactions between photons so that one is left with a fairly standard single-particle problem. This means that theoretical computations can provide very accurate descriptions and predictions of the properties of photons and therefore be very useful and complementary to experimental investigations. Another appealing aspect of Maxwell's equations is

that there is no fundamental length scale. If we ignore changes in the dielectric function with frequency, a photonic crystal designed at one length scale will have the same fractional gap as the crystal at any other length scale. Thus a given photonic crystal designed to operate at microwave frequencies, which is much easier to fabricate because of millimetre-scale feature sizes, can be used to deduce the properties of the same photonic crystal scaled down to submicrometre length scales.

To take full advantage of the potential of photonic crystals, it is necessary to develop an understanding and intuition of their photonic structure on the same level as we have for electrons in solids. Towards this end, it is natural to begin our discussion with an exploration of the physical origins of the photonic bandgap. This will illustrate how different dielectric lattice topologies can lead to gaps for different polarizations of light. We shall then proceed to investigate the photonic structure associated with line defects (waveguides) and point defects (microcavities). Waveguides in photonic crystals will provide a unique ability for guiding optical light in air, along narrow channels and around very tight bends, with no losses. Microcavities in photonic crystals will provide complete tunability in both defect frequency and symmetry; the latter leads to the new concept of an *orbital* angular momentum for the photon. Both will provide basic ingredients for using photonic crystals to control the spontaneous emission of atoms in materials. For simplicity, in all of these discussions, we shall concentrate on employing two-dimensionally periodic photonic crystals as generic examples. This is purely for ease of description and visualization. All of the conclusions drawn carry over to their more complex three-dimensional counterparts. While much of this discussion is based on theoretical modelling, several approaches have now been initiated to design and fabricate real three-dimensional photonic crystals.

The photonic bandgap

In the absence of external currents and sources, Maxwell's equations can be cast in the following simple form

$$\left\{\nabla \times \frac{1}{\epsilon(\mathbf{r})}\nabla \times\right\}\mathbf{H}(\mathbf{r}) = \frac{\omega^2}{c^2}\mathbf{H}(\mathbf{r}) \qquad (1)$$

where $\mathbf{H}(\mathbf{r})$ is the magnetic field of the photon, ω is its frequency, c is the speed of light and $\epsilon(\mathbf{r})$ is the macroscopic dielectric function. The solutions $\mathbf{H}(\mathbf{r})$ and ω are determined completely by the strength and symmetry properties of $\epsilon(\mathbf{r})$. If $\epsilon(\mathbf{r})$ is perfectly periodic, as in a perfect photonic crystal, the solutions are characterized by a wavevector $\mathbf{k}$ and a band index n. The region of all allowed wavevectors is called a Brillouin zone and the collection of all solutions is termed a band structure. We are interested in understanding the aspects of the dielectric geometry of a photonic crystal which lead to a complete bandgap in this band structure, that is, a region of frequencies with no allowed photon modes for any value of the wavevector $\mathbf{k}$ inside the Brillouin zone. For simplicity, we examine the band structure of a two-dimensionally periodic photonic crystal comprised of a square lattice of dielectric rods surrounded by air. This system is convenient from points of view of ease of theoretical calculation and ease of experimental fabrication and measurement.

In the top panel of Fig. 1 we illustrate a comparison between experiment[8] and theory[9] for the dispersion relations $\omega_n(\mathbf{k})$ of photons in a square lattice of alumina rods ($\epsilon = 8.9$). For the measurements, rods of diameter 0.74 mm and length 100 mm were arranged in a square array, as indicated in the inset, with a lattice constant $a = 1.87$ mm. Coherent microwave transient spectroscopy measurements were then performed for wavevectors $\mathbf{k}$ from (0,0) to (π/a,0), or equivalently from Γ to X, to measure the corresponding frequencies of the propagating photon. Because of the presence of a mirror symmetry plane perpendicular to the rods,

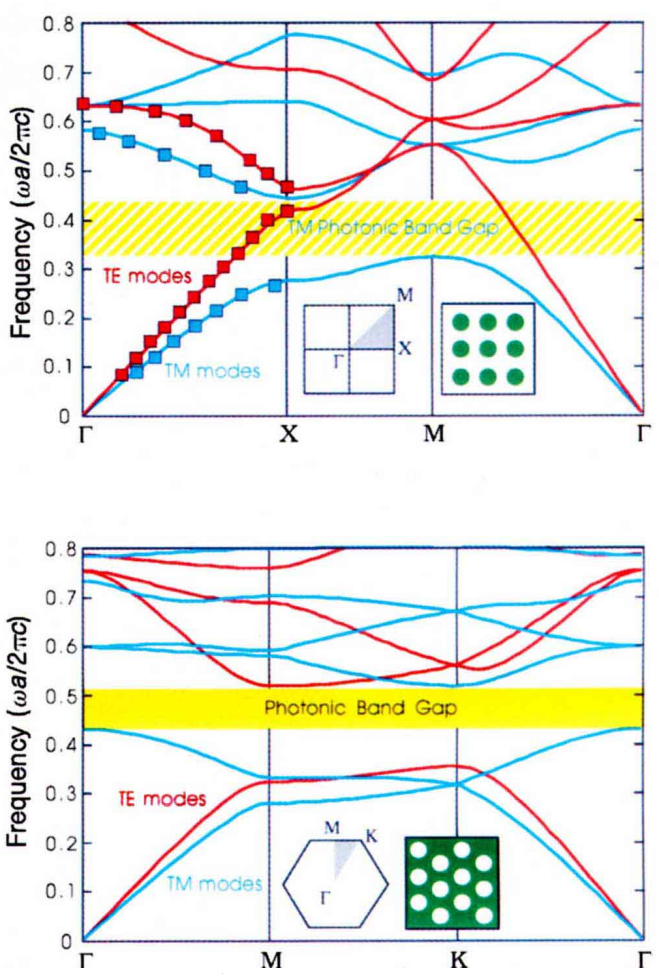

Figure 1 Top, photonic band structure for a square lattice of dielectric (ϵ = 8.9) rods in air with radius $r = 0.2a$, where a is the lattice constant. TM modes are shown in blue and TE modes in red. The solid lines are from theory and the squares represent experimental measurements along Γ to X from Robertson *et al.*[8] Bottom, photonic band structure for a triangular lattice of air cylinders (r = 0.48a) in dielectric (ϵ = 13). Note the presence of a complete photonic bandgap for both TE and TM polarizations in this case as shown by a solid yellow bar. In both panels high-dielectric material is indicated in green in the insets.

it is possible and convenient to decouple the photon modes into polarizations with transverse magnetic (TM) and transverse electric (TE) fields with respect to the plane normal.

The agreement between experiment and theory is excellent for both the TM and TE modes. We note also that for the TM modes there is an experimental indication of a large photonic bandgap between the first and second bands. This is substantiated by the calculation of the bands for the other high-symmetry directions of the Brillouin zone, as shown in Fig. 1. A complete bandgap does indeed exist between the first and the second TM bands. There is, however, no corresponding bandgap for the TE modes. It should be possible to explain such a significant fact.

If we examine the displacement field pattern associated with the lowest TM band we find that it is strongly concentrated in the dielectric regions. This is in sharp contrast to the field pattern associated with the second TM band which has most of its energy in the air regions. These statements have been quantified by calculation[9] of the fraction, f, of electrical energy inside the dielectric regions. For the modes at the X-point, for example, one obtains $f = 0.8$ and $f = 0.3$ for bands 1 and 2, respectively. The first band has most of its power in the dielectric regions and has a low

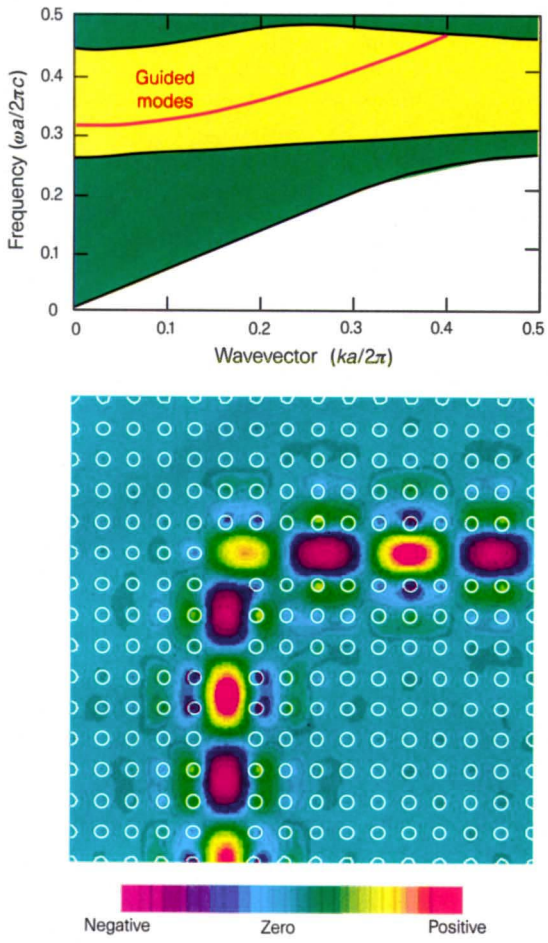

Figure 2 Top, projected photon bands for a waveguide in a square lattice of dielectric rods. The waveguide is formed by removing one row of rods from the otherwise perfect lattice and this creates a band of guided modes as shown in red. The green regions correspond to propagating modes in the bulk crystal and the yellow region corresponds to the photonic bandgap. Bottom, electric field of light propagating down a waveguide with a sharp bend carved out of a square lattice of dielectric rods. The white circles indicate the positions of the rods.

frequency; the second has most of its power in the air region, and has a much higher frequency.

The fractions f for the TE modes do not contrast as strongly. At the X-point, for example, one finds $f = 0.2$ and $f = 0.1$ for the first and second bands, respectively. In this case, both modes have significant amplitude in the air regions, raising their frequencies. They have no other choice; the field lines must be continuous so they are forced to penetrate the air regions. This is the origin of the small values of f and explains the absence of a bandgap for the TE modes. Note that the vector nature of the photon field is central to this argument. The scalar displacement field along the rods of the TM modes can be localized within the rods, but the continuous field lines of the TE modes are compelled to penetrate the air regions to connect neighbouring rods. As a result, consecutive TE modes do not exhibit markedly different f factors, and bandgaps do not appear.

Although we will not discuss it any further here, it is interesting to note that exactly the opposite behaviour is found for TE and TM modes in the case of a crystal with a connected dielectric lattice: an in-depth discussion of this and other aspects of the nature of the photonic bandgap is given is ref. 9. We shall only state the general rule of thumb: TM band gaps are favoured in a lattice of isolated high-ϵ regions, and TE gaps are favoured in a connected lattice.

This rule of thumb may be used to design a photonic crystal that has a gap for both TE and TM modes. The approach is a sort of compromise: crystals with high-ϵ regions that are both practically isolated and linked by narrow veins. An example of such a system is the triangular lattice of air columns shown in the bottom panel of Fig. 1. A complete photonic bandgap clearly exists for both TE and TM polarizations[10,11]. Such a gap has recently been observed experimentally in the near-infrared regime along the Γ to K and Γ to M directions for deeply-etched bulk structures[12] and for thin integrated waveguide structures[13].

It is also possible to find photonic-crystal structures which are not connected, yet exhibit a complete photonic bandgap in the higher-lying bands. This can occur when there is more than one 'dielectric-atom' per lattice constant. An example is the honeycomb lattice of dielectric rods[1,14]. These types of crystal have the advantage that the larger value of the mid-gap frequency results in a larger value of the minimum feature size. This can be a very important issue in fabrication.

It turns out to be quite typical that the bands above and below a bandgap can be distinguished by where the power lies—in the high-ϵ regions, or in the low-ϵ (usually air) regions. For this reason it is convenient to refer to the band above a photonic bandgap as the 'air band' and the band below a gap as the 'dielectric band'. This is in direct analogy with the use of the terms 'conduction band' and 'valence band' for the electronic band structure of semiconductors.

The waveguide

Once we have a photonic crystal with a gap we can introduce a defect to attempt to trap or localize the light. If we use a line defect, we can also guide light from one location to another. The basic idea is to carve a waveguide out of an otherwise-perfect photonic crystal. Light that propagates in the waveguide with a frequency within the bandgap of the crystal is confined to, and can be directed along, the waveguide. This is a truly novel mechanism for the guiding of light. Traditionally, optical light can be guided without losses within dielectric waveguides such as fibre-optic cables, which rely exclusively on total internal reflection. But, if a fibre optic curves tightly, the angle of incidence is too large for total internal reflection to occur, so light escapes at the corners and is lost. Photonic crystals, on the other hand, continue to confine light even around tight corners.

To illustrate these ideas, we turn again to the square lattice of dielectric rods as a simple example and consider only the TM modes. In the top panel of Fig. 2 we plot the projected bands along the direction of propagation for a waveguide formed by removing one row of rods. The green regions correspond to states that can propagate through the crystal. The band of states within the gap region corresponds to guided modes, which can travel freely within the narrow waveguide channel.

Once light is induced to travel along the waveguide it really has nowhere else to go. An intriguing aspect of photonic-crystal waveguides is that they provide the means to guide optical light, tractably and efficiently, through narrow channels of air. As the frequency of the guided mode lies within the photonic bandgap, the mode is forbidden to escape into the crystal. The primary source of loss can only be reflection back out of the waveguide entrance. This suggests that we may use a photonic crystal to guide light around tight corners. This is also shown in the bottom panel of Fig. 2, as obtained from transmission simulations by Mekis *et al.*[15]. Even though the radius of curvature of the 90° bend is zero, 98% of the power in the light that goes in one end comes out of the other. This should be contrasted with 30% power transmission in an analogous dielectric waveguide[15]. Making very sharp lossless bends in waveguides which operate at 1.5 μm is of great practical importance for enabling miniaturization of optoelectronic components and circuits.

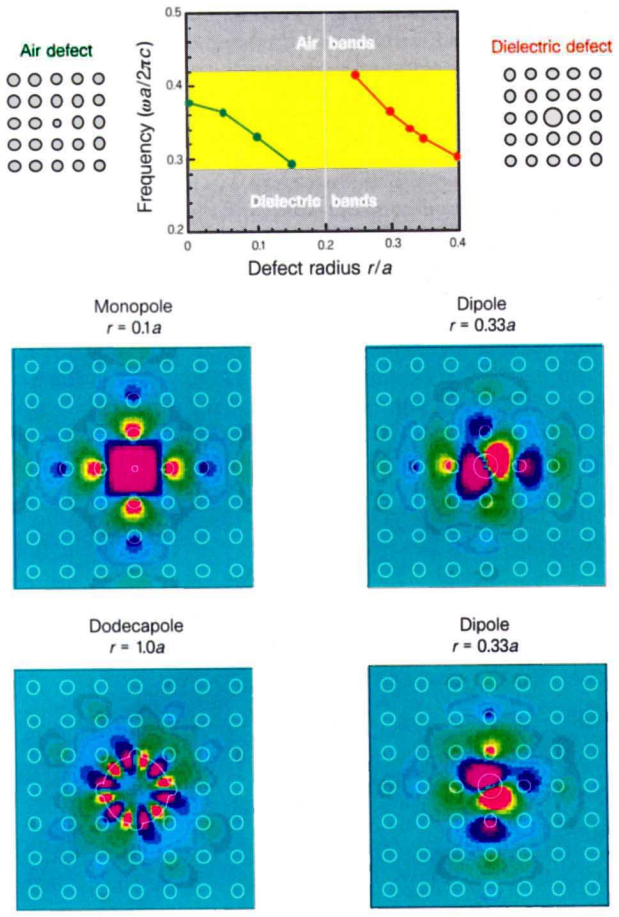

Figure 3 Top, localized states in the gap for a defect formed by varying the radius r of a single rod in the square lattice of dielectric rods with lattice constant a. The case where there is no defect corresponds to $r = 0.2a$, while the case of a vacancy corresponds to $r = 0$. Bottom panels, electric field patterns associated with selected defect states as indicated. The colour coding is the same as in the bottom panel of Fig. 2.

The cavity

One can also create imperfections to trap light at a point within the crystal. One class of imperfections of this type involves changing the dielectric medium in some local region of the crystal, deep within its bulk. As a simple example, consider making a change to a single 'dielectric atom' by modifying its dielectric constant, modifying its size, or simply removing it from the crystal. The top panel of Fig. 3 shows the consequence of creating a vacancy in the square lattice of rods (a vacancy corresponds to a defect radius of $r = 0$). A defect state does indeed appear in the photonic bandgap leading to a strongly localized state. By removing a rod from the lattice, we effectively create a cavity which is surrounded by reflecting walls. If the cavity has the proper size to support a mode in the bandgap, then light cannot escape, and we can pin the mode to the defect.

If the defect involves removal of dielectric (an 'air defect' as in the case of the vacancy) then the cavity mode evolves from the dielectric band and can be made to sweep across the gap by adjusting the amount of dielectric removed. Similarly, if the defect involves the addition of extra dielectric material (a 'dielectric defect') then the cavity mode drops from the air band. As shown in the top panel of Fig. 3, in both cases the defect state can be tuned to lie anywhere in the gap.

Apart from tuning the frequency, one also has some control over the symmetry of the localized photonic state. For example, the middle and bottom panels of Fig. 3 show the symmetries of the localized photon mode for three different values of the defect radius. For the case of $r = 1.0a$ we find a field pattern that is very reminiscent of the 'whispering gallery' mode observed in microdisk laser cavities[16].

The very specific symmetry associated with each photon mode translates into an orbital angular momentum for each photon mode which can exist in addition to its intrinsic spin angular momentum. This is a very intriguing notion that can have spectacular consequences in the selection rules of electronic transition rates, as discussed below. Further information about air and dielectric defects can be found in refs 17–25.

The flexibility in tuning the symmetry, frequency and localization properties of defects makes photonic crystals a very attractive medium for the design of novel types of filters, couplers, lasers, light-emitting diodes (LEDs) and so on[16,26]. In the case of laser or LED cavities, photonic crystals provide a particularly unique capability—the control of spontaneous emission.

Spontaneous emission is the natural tendency for an excited atom to 'fall' to a state of lower energy while releasing its energy in the form of emitted radiation. This process, which occurs independently for each atom in a crystal, is at the heart of every light-emitting device used in the optoelectronic industry. LEDs, for example, emit light from the radiative recombination of electrons and holes in a forward-biased p–n junction. Moreover, by increasing the applied voltage, the number of electron–hole pairs in the junction region can become sufficiently large for stimulated emission (that is, the emission induced by other photons) to become prevalent. The junction may then be used as a diode laser.

The ability to control spontaneous emission could have profound consequences for many optoelectronic devices. The rate at which atoms decay depends on the coupling between the atom and the photon, and also on the density of electromagnetic modes available for the emitted photon. Photonic crystals could be used to control each of these two elements independently, simply by changing the properties of the defect states. For instance, the coupling between the atom and the photon involves an integral over all space of the initial and final states of the atom, and of the vector-potential associated with the photon. In the usual dipole approximation, one assumes a uniform vector-potential in the vicinity of each atom, which leads to the standard 'selection rules' for atomic transitions as illustrated in the left panel of Fig. 4. But in the case of a photonic crystal, we can engineer the vector-potential to have specific orbital symmetry. By doing so, transitions that are usually allowed could be made forbidden, and more interestingly, electronic transitions that were previously forbidden could now be made allowed, by judiciously choosing the orbital angular momentum of the defect-state photon, as illustrated in the right panel of Fig. 4. This latter case would be possible if the wavelength of the electron and that of the photon were designed to be of the same order. A synergy between quantum-well and photonic-crystal technologies might be one approach for fabricating systems for which this phenomenon could be measured experimentally.

In addition to changing the coupling between the atom and the photon, the rate of spontaneous emission could also be affected by changing the density of allowed states. If we assume a non-zero coupling between the atom and the photon, the 'natural' rate of emission, in free space, is proportional to the free-photon density of states per unit volume, D_f, which scales as

$$D_f \approx \frac{1}{\omega}\frac{1}{\lambda^3} \qquad (2)$$

where ω is the frequency of the transition and λ the wavelength of light. If the system is a photonic crystal with a photonic bandgap around ω, there are no allowed modes to couple to and spontaneous emission is severely inhibited. Conversely, if the photonic crystal is

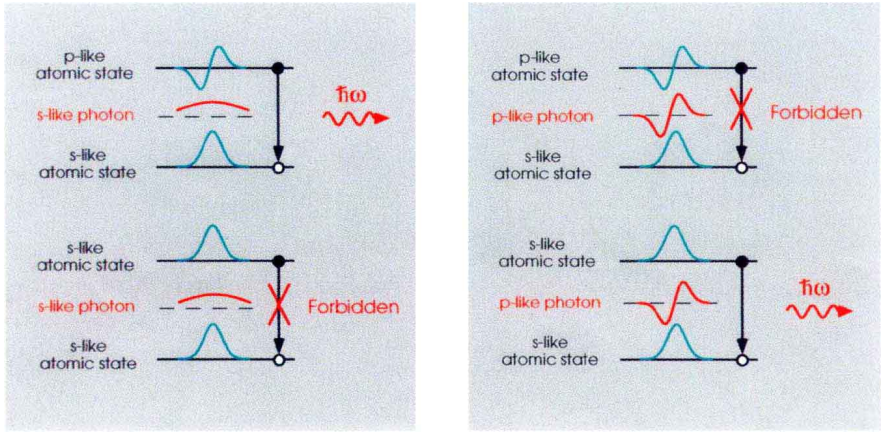

Figure 4 Schematic representation of allowed and forbidden optical transitions for an electron between two atomic states. The symmetry of the orbital angular momentum for the atomic states is shown in blue; the symmetry of the orbital angular momentum of the photon state is shown in red. The panel on the left corresponds to the usual 'selection rules' for atomic transitions. The panel on the right indicates novel selection rules possible using photonic crystals.

designed to have a point defect with a localized, or more generally, a resonant state at ω, then the emission rate could be enhanced dramatically by the increase in the density of final states. An estimate of this enhancement can be obtained from the following simple argument. The density of states per unit volume for the resonance, D_r, will scale as

$$D_r \approx \frac{1}{\Delta\omega}\frac{1}{\Omega} \tag{3}$$

where $\Delta\omega$ is the frequency width of the resonance and Ω is its effective spatial volume. The enhancement factor is then given roughly by

$$\frac{D_r}{D_f} \approx \frac{\omega}{\Delta\omega}\frac{\lambda^3}{\Omega} = \frac{Q}{(\Omega/\lambda^3)} \tag{4}$$

where $Q \equiv (\omega/\Delta\omega)$ is the quality factor of the cavity. Thus high Q and small spatial volumes can lead to significant enhancement of spontaneous emisison. As the smallest volume Ω must be of the order of λ^3, the largest enhancement will be of the order of Q. Cavities whose spatial volume is of the order of the wavelength of light are called microcavities.

Experimentalists have begun exploring the possibilities of fabricating these microcavities with silicon-based materials and with III–V semiconductor-based materials at micrometre and submicrometre length scales. An exciting new design of a microcavity involves an integrated waveguide–microcavity configuration[27], two embodiments of which have recently been successfully fabricated, as shown in the scanning electron micrographs of Fig. 5 (J. Forezi, L. Kimerling and H. Smith, and K. Lim, G. Petrich and L. Kolodziejski, unpublished results). The basic design employs a one-dimensional photonic crystal to confine light in the direction along the waveguide and near the defect at the centre, and total internal reflection to confine light in the transverse directions. The structure in the top panel of Fig. 5 corresponds to a monorail-like geometry fabricated using Si and SiO_2 with electron-beam lithography. The structure in the bottom panel is a novel suspended air-bridge geometry fabricated using GaAs and AlGaAs with a photolithographic technique. In each case, the defect at the centre sustains only one cavity mode whose field patterns are localized to within half a wavelength along the guide and decay rapidly into the air regions. Calculations of the Q for such cavity modes, even for non-optimized geometries, are as high as 10^4 (refs 22, 28). Moreover, and indeed very importantly, we expect the properties of such cavities to be rather robust with respect to random defects. Such disorder will typically arise during fabrication, and the amount of disorder will of course depend on the minimum feature sizes and the fabrication technique. Calculations[29] for a structure with surface disorder whose average size is as large as $\pm 10\%$ of the width of the waveguide, reveal that the Q drops by only 30%. There are two basic reasons for this. First, the wavelength of the mode is significantly larger than the characteristic size of the defects. Second,

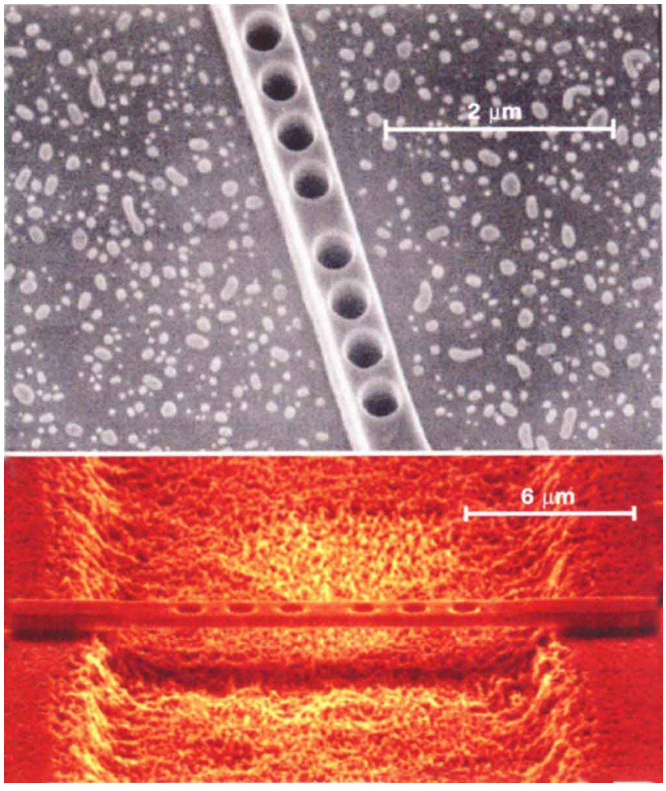

Figure 5 Scanning electron micrographs of two embodiments of a waveguide-integrated photonic crystal microcavity. Top, the monorail geometry fabricated using Si on SiO_2 with electron-beam lithography (J. Foresi, L. Kimerling and H. Smith, unpublished results) . Bottom, the air-bridge geometry fabricated using GaAs on AlGaAs with a photolithographic technique (K. Lim, G. Petrich and L. Kolodziejski, unpublished results).

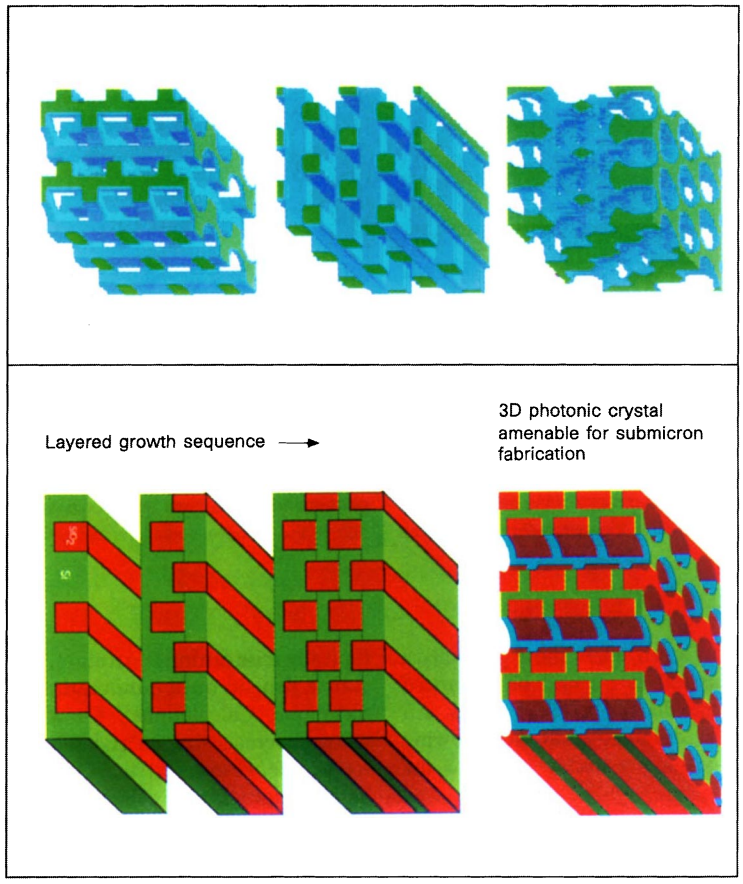

Figure 6 Photonic crystal structures with 3D periodicity (see text for details). Left panel: top, 'Yablonovite' (ref. 30); middle, structure developed by Ho *et al.* (ref. 33); bottom, structure developed by Fan *et al.* (ref. 37). Right panel: lower three structures, schematic growth sequence for the Fan *et al.* structure; top, final structure obtained after etching vertical holes.

most of the energy of the mode is concentrated in the middle of the cavity and away from the surface. This makes the effect of the surface roughness much less significant for this structure than, say, for microdisks in which the high-Q modes propagate along the boundary of the disks[16].

The three-dimensional photonic crystal

The first three-dimensionally (3D) periodic photonic crystal possessing a complete bandgap was fabricated by Yablonovitch[30] in 1991 for the microwave regime. The fabrication technique involved covering a slab of dielectric with a mask consisting of a triangular array of holes. Each hole was then drilled three times along (110)-type directions. The resulting structure (known affectionately as 'Yablonovite') is shown at the top of the left panel in Fig. 6. Since then, several other 3D photonic-crystal designs have appeared that offer complete photonic bandgaps[31–34].

Of these, the Ho *et al.* structure[33] (shown in the middle of the left panel of Fig. 6) is the smallest 3D photonic crystal with an experimentally demonstrated complete bandgap to be manufactured to date. Özbay *et al.*[35] have used a technique of stacking thin micromachined (110) silicon wafers to fabricate these photonic crystals for wavelengths approaching 600 μm.

The ultimate goal for optoelectronic applications is to design and fabricate 3D photonic crystals at an operating wavelength of 1.5 μm. This is certainly not a trivial task. Most recently, Scherer and coworkers[36] performed a set of experiments to demonstrate the exciting possibility of fabricating 'Yablonovite' at 1.5 μm, using electron-beam lithography to 'drill' the (110)-type air channels. The first several layers of 'Yablonovite' have been created in this fashion.

A new class of photonic crystals, designed specifically to be amenable for fabrication at submicrometre length scales and to possess a large and complete bandgap, has recently been introduced by Fan *et al.*[37]. One embodiment of this type of photonic crystal is shown at the bottom of the left panel of Fig. 6. The crystal is designed to be fabricated in a layered fashion, using two different dielectric materials (for example, Si and SiO_2), with a series of non-intersecting air channels etched at normal incidence through the top surface after growth is completed. (The presence of non-intersecting air channels was actually a constraint imposed on the design and deemed important for easily maintaining high quality during fabrication.) To create a crystal with a larger dielectric contrast (and consequently a larger bandgap), one of the two dielectric materials can be chosen so that it can be removed at the end by selective etching. The sequence of 'growth' steps illustrated in the right panel of Fig. 6 are shown to help the visualizaiton of the basic elements that make up the crystal structure. First, a layer of Si is deposited on a substrate of choice and grooves are etched into the Si layers as shown. The grooves run normal to the page and are arranged in a periodic array. The grooves are then filled with SiO_2 and another Si layer is grown on the previous layer. Long grooves are again etched (which now extend into the first layer) and again back-filled with SiO_2. Repetition of this procedure generates the basic bulk structure of the photonic crystal. The final step is to etch an array of air channels into the top surface of the structure, at normal incidence.

The design of this structure has many degrees of freedom which can be used to optimize the size of the bandgap. Using a dielectric constant of 12.096 for Si at 1.5 μm and 2.084 for silica at the same

frequency gives an optimized complete photonic bandgap of about 14%. A very significant improvement can be made by simply removing the oxide. The resulting photonic-crystal structure is then predicted to possess a sizeable 23% gap[37]. Moreover, calculations of the predicted transmission spectra for this structure reveal that with a photonic-crystal thickness of only seven layers one can achieve four orders of magnitude reduction in transmission through the bandgap (J. Weitz, S.F., P.R.V. and J.D.J., unpublished results). This structure is currently being fabricated at the 4.5 μm length scale by Kolodziejski, Reif and co-workers at MIT, using optical lithography. Two layers of the photonic crystal have already been successfully grown.

A very new and exciting approach to the design and fabrication of submicrometre 3D photonic crystals involves the creation of a periodic lattice of isolated metallic regions within a dielectric host[38]. Such 3D metallodielectric photonic crystals have been studied theoretically[39–42] and can be shown[42] to have enormous omnidirectional bandgaps approaching 80%. As the metallic regions are not connected and light tends to be attracted away from the metal towards the dielectric, it is hoped that the effects of the losses expected at optical frequencies may not be too important. Efforts are currently underway at the MIT-Lincoln Laboratory to fabricate and measure the losses and other properties of these metallodielectrics.

The challenge

Photonic crystals offer the possibility of controlling and manipulating light by opening a gap in the density of electromagnetic states within a given range of frequencies. Whereas perfect crystals may be valuable for the fabrication of devices such as high-efficiency light-emitting diodes and 3D mirrors, the introduction of a defect in the crystal, either locally or in an extended region, will allow us to generate electromagnetic states with specific properties. The ability to custom-design a state may prove to be essential in the fabrication of laser sources in frequency ranges yet unseen, and novel optical devices such as switches, modulators, filters and interconnects.

From its beginning less than ten years ago, research in the field of photonic crystals has been advancing at high speeds. To maintain the same rate of progress in the next ten years, it will be necessary for experimentalists to overcome the challenges associated with the fabrication of small intricate three-dimensional periodic structures with feature sizes of less than one μm. Only then will photonic crystals be able to fulfill our expectations. □

J. D. Joannopoulos, P. R. Villeneuve and Shanhui Fan are at the Massachusetts Institute of Technology, Cambridge, Massachusetts 02139, USA.

1. Joannopoulos, J., Meade, R. & Winn, J. *Photonic Crystals* (Princeton Press, Princeton, NJ, 1995).
2. Yablonovitch, E. Inhibited spontaneous emission in solid-state physics and electronics. *Phys. Rev. Lett.* **58,** 2059–2062 (1987).
3. John, S. Strong localization of photons in certain disordered dielectric superlattices. *Phys. Rev. Lett.* **58,** 2486–2489 (1987).
4. John, S. Electromagnetic absorption in a disordered medium near a photon mobility edge. *Phys. Rev. Lett.* **53,** 2169–2172 (1984).
5. Anderson, P. W. Absence of diffusion in certain random lattices. *Phys. Rev.* **109,** 1492–1505 (1958).
6. Drake, M. & Genack, A. Observation of nonclassical optical diffusion. *Phys. Rev. Lett.* **63,** 259–262 (1989).
7. Genack, A. & Garcia, N. Observation of photon localization in a three-dimensional disordered system. *Phys. Rev. Lett.* **66,** 2064–2067 (1991).
8. Robertson, W. *et al.* Measurement of photonic band structure in a two-dimensional periodic dielectric array. *Phys. Rev. Lett.* **68,** 2023–2026 (1992).
9. Meade, R., Brommer, K., Rappe, A. & Joannopoulos, J. Nature of the photonic band gap: some insights from a field analysis. *J. Opt. Soc. Am. B* **10,** 328–332 (1993).
10. Meade, R., Brommer, K., Rappe, A. & Joannopoulos, J. Existence of a photonic band gap in two dimensions. *Appl. Phys. Lett.* **61,** 495–497 (1992).
11. Villeneuve, P. & Piché, M. Photonic band gaps in two-dimensional square and hexagonal structures. *Phys. Rev. B* **46,** 4969–4972 (1992).
12. Grüning, U., Lehmann, V., Ottow, S. & Busch, K. Macroporous silicon with a complete two-dimensional photonic band gap centered at 5 μm. *Appl. Phys. Lett.* **68,** 747–749 (1996).
13. Krauss, T., De La Rue, R. & Band, S. Two-dimensional photonic bandgap structures operating at near-infrared wavelengths. *Nature* **383,** 699–702 (1996).
14. Cassagne, D., Jouanin, C. & Bertho, D. Hexagonal photonic-band-gap structures. *Phys. Rev. B* **53,** 7134–7142 (1996).
15. Mekis, A. High transmission through sharp bends in photonic crystal waveguides. *Phys. Rev. Lett.* **77,** 3787–3790 (1996).
16. Slusher, R. Semiconductor microlasers and their applications. *Opt. Photonics News* **4(2),** 8–17 (1993).
17. Meade, R., Brommer, K., Rappe, A. & Joannopoulos, J. Photonic bound states in periodic dielectric materials. *Phys. Rev. B* **44,** 13772–13774 (1991).
18. Yablonovitch, E. Donor and acceptor modes in photonic band structure. *Phys. Rev. Lett.* **67,** 3380–3383 (1991).
19. McCall, S., Platzman, P., Dalichaouch, R., Smith, D. & Schultz, S. Microwave propagation in two-dimensional dielectric lattices. *Phys. Rev. Lett.* **67,** 2017–2020 (1991).
20. Leung, K. Defect modes in photonic band structures: a Green's function approach using vector Wannier functions. *J. Opt. Soc. Am. B* **10,** 303–306 (1993).
21. Maradudin, A. & McGurn, A. in *Photonic Band Gaps and Localizaiton* (ed. Soukoulis, C.) 247–268 (Plenum, New York, 1993).
22. Fan, S. *et al.* Guided and defect modes in periodic dielectric waveguides. *J. Opt. Soc. Am. B* **12,** 1267–1272 (1995).
23. Sigalas, M., Soukoulis, C., Chan, C. & Ho, K. in *Photonic Band Gap Materials* (ed. Soukoulis, C.) 173–202 (Kluwer, Dordrecht, 1996).
24. Birks, T., Atkin, D., Wylangowski, G., Russel, P. & Roberts, P. *Photonic Band Gap Materials* (ed. Soukoulis, C.) 437–444 (Kluwer, Dordrecht, 1996).
25. Villeneuve, P., Fan, S. & Joannopoulos, J. Microcavities in photonic crystals: mode symmetry, tunability, and coupling efficiency. *Phys. Rev. B* **54,** 7837–7842 (1996).
26. Meade, R. *et al.* Novel applications of photonic band gap materials: low loss bends and high Q cavities. *J. Appl. Phys.* **75,** 4753–4755 (1994).
27. Villeneuve, P. *et al.* Air-bridge microcavities. *Appl. Phys. Lett.* **67,** 167–169 (1995).
28. Chen, J., Haus, H., Fan, S. Villeneuve, P. & Joannopoulos, J. Optical filters from photonic band gap air bridges. *IEEE J. Lightwave Tech.* **14,** 2575–2580 (1996).
29. Joannopoulos, J. The almost-magical world of photonic crystals. *Braz. J. Phys.* **26,** 58–67 (1996).
30. Yablonovitch, E., Gmitter, T. & Leung, K. Photonic band structure: the face-centered-cubic case employing nonspherical atoms. *Phys. Rev. Lett.* **67,** 2295–2298 (1991).
31. Chan, C., Ho, K. & Soukoulis, C. Photonic band-gaps in experimentally realizable periodic structures. *Europhys. Lett.* **16,** 563–568 (1991).
32. Sözüer, H. & Haus, J. Photonic bands: simple-cubic lattice. *J. Opt. Soc. Am. B* **10,** 296–302 (1993).
33. Ho, K., Chan, C., Soukoulis, C., Biswas, R. & Sigalas, M. Photonic band gaps in three dimensions: new layer-by-layer periodic structures. *Solid State Commun.* **89,** 413–416 (1994).
34. Sözüer, H. & Dowling, J. Photonic band calculations for woodpile structures. *J. Mod. Opt.* **41,** 231–239 (1994).
35. Özbay, E. *et al.* Micromachined millimeter-wave photonic band-gap crystals. *Appl. Phys. Lett.* **64,** 2059–2061 (1994).
36. Cheng, C. & Scherer, A. Fabrication of photonic band-gap crystals. *J. Vac. Sci. Technol. B* **13,** 2696–2700 (1995).
37. Fan, S., Villeneuve, P., Meade, R. & Joannopoulos, J. Design of three-dimensional photonic crystals at submicron lengthscales. *Appl. Phys. Lett.* **65,** 1466–1468 (1994).
38. Brown, R. & McMahon, O. Large electromagnetic stop bands in metallodielectric photonic crystals. *Appl. Phys. Lett.* **67,** 2138–2140 (1995).
39. McGurn, A. & Maradudin, A. Photonic band structures of two- and three-dimensional periodic metal or semiconductor arrays. *Phys. Rev. B* **48,** 17576–17579 (1993).
40. Pendry, J. Photonic band structures. *J. Mod. Opt.* **41,** 209–229 (1994).
41. Sigalas, M., Chan, C., Ho, K. & Soukoulis, C. Metallic photonic band-gap materials. *Phys. Rev. B* **52,** 11744–11751 (1995).
42. Fan, S., Villeneuve, P. & Joannopoulos, J. Large omnidirectional band gaps in metallodielectric photonic crystals. *Phys. Rev. B* **54,** 11245–11251 (1996).

Acknowledgements. The work was supported by the US NSF through the MRSEC at MIT.

Correspondence and requests for materials should be addressed to J.D.J.